

CONTINUING A *CHANDRA* SURVEY OF QUASAR RADIO JETS

J. M. Gelbord, H. L. Marshall

Massachusetts Institute of Technology

77 Massachusetts Ave., Cambridge, MA 02139, U.S.A.

JONATHAN@SPACE.MIT.EDU, HERMANM@SPACE.MIT.EDU

D. A. Schwartz, D. M. Worrall, M. Birkinshaw

DAS@HEAD-CFA.HARVARD.EDU, D.WORRALL@BRISTOL.AC.UK, MARK.BIRKINSHAW@BRISTOL.AC.UK

J. E. J. Lovell, D. L. Jauncey, E. S. Perlman

JIM.LOVELL@CSIRO.AU, DAVID.JAUNCEY@CSIRO.AU, PERLMAN@JCA.UMBC.EDU

D. W. Murphy, R. A. Preston

DWM@SGRA.JPL.NASA.GOV, ROBERT.A.PRESTON@JPL.NASA.GOV

Abstract

We are conducting an X-ray survey of flat spectrum radio quasars (FSRQs) with extended radio structures. We summarize our results from the first stage of our survey, then we present findings from its continuation.

We have discovered jet X-ray emission from 12 of our first 20 *Chandra* targets, establishing that strong 0.5–7.0 keV emission is a common feature of FSRQ jets. The X-ray morphology is varied, but in general closely matches the radio structure until the first sharp radio bend. In the sources with optical data as well as X-ray detections we rule out simple synchrotron models for X-ray emission, suggesting these systems may instead be dominated by inverse Compton (IC) scattering. Fitting models of IC scattering of cosmic microwave background photons suggests that these jets are aligned within a few degrees of our line of sight, with bulk Lorentz factors of a few to ten and magnetic fields a bit stronger than 10^{-5} G.

In the weeks prior to this meeting, we have discovered two new X-ray jets at $z > 1$. One (PKS B1055+201) has a dramatic, $20''$ -long jet. The other (PKS B1421–490) appears unremarkable at radio frequencies, but at higher frequencies the jet is uniquely powerful: its optically-dominated, with jet/core flux ratios of 3.7 at 1 keV and 380 at 480 nm.

1 Introduction

A quarter century after the discovery of extragalactic X-ray jets (Schreier et al., 1979), many fundamental

questions remain unanswered. Even the process responsible for the high-energy emission remains a subject of debate: in some instances the radio synchrotron continuum appears to extend to the X-ray band (e.g., knot A1 of 3C273: Marshall et al., 2001), while in others inverse Compton (IC) scattering best describes the observations (e.g., PKS 0637–752: Schwartz et al., 2000). In order to assess the distribution of high energy emission mechanisms among quasar jets, and to use this information to determine the range of physical conditions, we are conducting a multi-wavelength survey of a large sample of flat spectrum quasars (FSRQs; defined as quasars with core radio spectral index values $\alpha < 0.5$, where $F_\nu \propto \nu^{-\alpha}$) selected by their extended ($> 2''$) flux at 5 GHz (Marshall et al., 2005). Brief *Chandra* exposures are used to detect X-ray bright jets and to identify candidates for follow-up observations; radio and optical observations allow multi-waveband morphological comparisons and fill in the jet spectral energy distribution (SED), which in turn constrain the emission models.

2 The initial survey

The preliminary survey consists of twenty 5 ks ACIS observations made during *Chandra* cycle 3. These X-ray data are supplemented with new radio maps made with the Australia Telescope Compact Array (ATCA) and Very Large Array, and *Magellan* optical images, all with sub-arcsecond resolution. The twenty targets are drawn from our full sample of 56 FSRQs, including ten targets from a flux-limited subsample and ten from a morphologically-selected extension to this sample.

We detect jets in 12 of the *Chandra* sources, indicating that strong X-ray emission is a common feature of quasar jets. We consider this discovery rate to be a lower limit for the incidence of X-ray jets because the detection rate among the flux-limited subsample is higher (8 out of 10), suggesting that X-ray jets may be present but below our detection threshold in some of our fainter targets. All of the detected jets are one-sided, but there is considerable variety in their details (Fig. 1). X-ray hotspots are found to coincide with radio knots, which is suggestive of a direct connection between the low- and high-energy emission mechanisms. This is consistent with both of the favored models for jet emission: the X-rays either represent the synchrotron emission of the highest-energy electrons, or IC scattering by the low-energy end of the synchrotron-emitting electron population. When the radio jet bends sharply the X-ray jet usually ends or weakens dramatically, consistent with either a deceleration/depletion of the highest energy electrons in the synchrotron picture or a change to a less-favored beaming angle in the IC model (Marshall et al., 2005).

As of January 2004, only six of the X-ray bright systems had yet been observed with *Magellan*, and none of these jets were detected. The optical flux upper limits rule out simple synchrotron models, which predict a flat or concave-down spectrum unless a second population of electrons is invoked (Harris & Krawczynski, 2002; but see Dermer & Atoyan 2002 for an alternative synchrotron model with a single electron population extending into the Klein-Nishina regime). In the case of PKS 1202–262, the optical fluxes are at least 2–3 magnitudes below the interpolation between the radio and X-ray fluxes (Fig. 2), strongly suggesting the IC model. If we apply jet models of IC scattering off the cosmic microwave background (Tavecchio et al., 2000; Celotti, Ghisellini & Chiaberge, 2001), we obtain magnetic fields of order $B \sim 10^{-5}$ G, bulk Lorentz factors up to $\Gamma \sim 10$, kinetic powers of 10^{46} – 10^{47} erg s $^{-1}$, and alignments close to our line of sight implying deprojected lengths of hundreds of kpc (Schwartz et al., 2003).

3 The latest results

3.1 January 2004 *Chandra* observations

Two new sources observed with *Chandra* in the weeks prior to this meeting have revealed remarkable X-ray structures (Fig. 3). The X-rays from PKS 1055+201

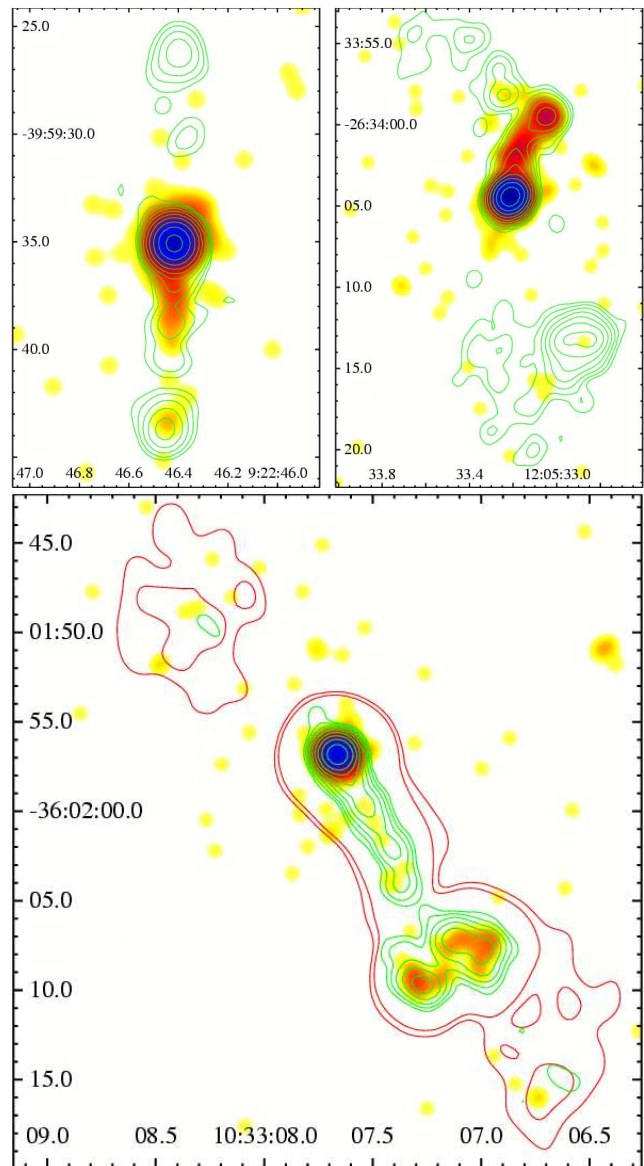


Figure 1: *Chandra* 0.5–7.0 keV X-ray images of PKS 0920–397, PKS 1202–262 and PKS 1030–357 (clockwise from top left) with ATCA radio contours overlaid. Images and contours have been convolved to matching 1.2'' FWHM resolution. All contours start at $5 \times$ the background RMS level of the respective radio maps; green contours represent 8.6 GHz data and the two outermost (red) contours around 1030–357 illustrate the larger-scale structure using the lowest levels from the 4.8 GHz map. The upper two images are representative in that the X-rays follow the radio jet where it is straight or bends modestly, but end where the radio jet bends sharply; the X-ray/radio flux ratio declines along the jet of 0920–397 and stays relatively constant along the inner 6'' of 1202–262. PKS 1030–357 is unusual in that the X-rays are barely detected in the inner jet, intensify at the first knot and remain strong through what appears to be two sharp bends in the radio jet.

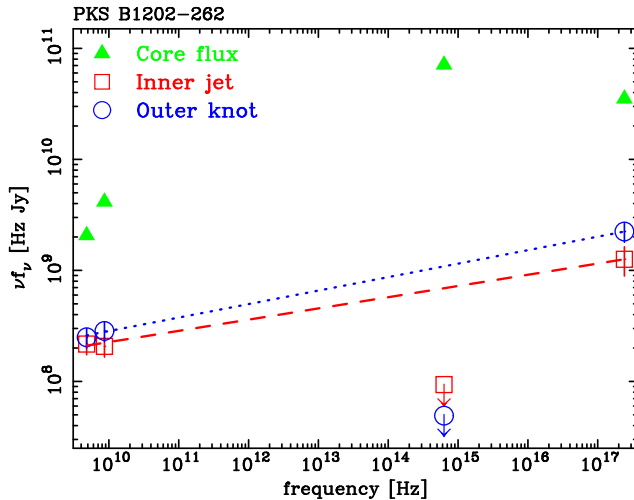
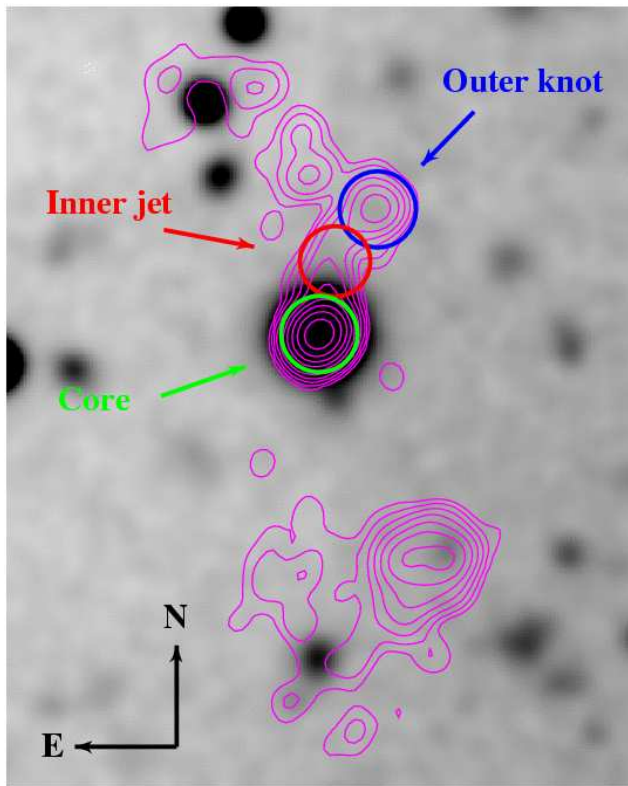


Figure 2: *Top panel:* *Magellan* optical (SDSS g') image of PKS 1202–262 with ATCA 8.6 GHz radio contours overlaid. *Bottom panel:* Radio–optical–X-ray SED plot for the three regions labeled on the image. Simple power law interpolations for the inner jet and outer knot are sketched in as dashed and dotted lines, respectively.

(observed 2004 Jan. 19) trace a long, arcing radio jet, terminating at the near side of an extended radio feature 21.3'' from the core. This jet brightens as it approaches the radio feature, possibly indicating the diffusion of shock accelerated electrons back down the

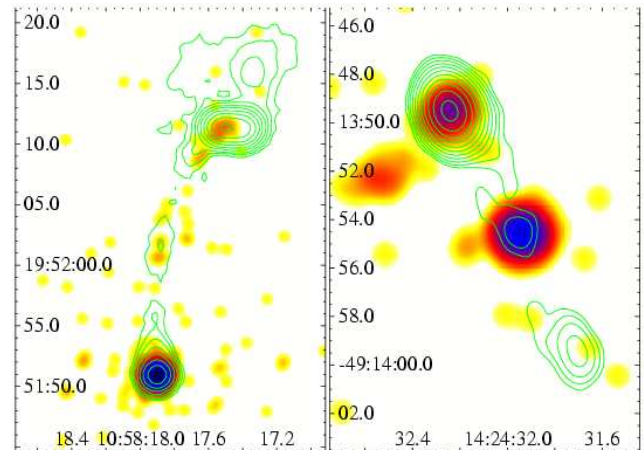


Figure 3: *Chandra* 0.5–7.0 keV images of PKS B1055+201 (*left*) and PKS B1421–490 (*right*); the former is shown with 1.4 GHz radio contours, the latter has 8.6 GHz contours.

jet. PKS 1421–490 (observed 2004 Jan. 16) is the first system we’ve found to be dominated at high frequencies by its jet. The unresolved X-ray feature 5.8'' SW of the radio core provides 79% of the 0.5–7.0 keV flux.

3.2 The incredible jet of PKS 1421–490

PKS 1421–490 is the only member of our sample without a previously-identified optical counterpart. We observed the field with *Magellan* in the Sloan Digital Sky Survey (SDSS) g' , r' and i' filters, identifying a 24th magnitude source within 0.3'' of the radio core (Fig. 4). The dereddened colors of this source are consistent with quasars at $1 \lesssim z \lesssim 2$, suggesting that 1421–490 is one of the more distant members of our sample (Gelbord & Marshall, 2005).

Coinciding with the strong X-ray peak is an unresolved source that is ~ 300 times brighter than the optical core. In no other known quasar system does the jet so thoroughly overwhelm the core in the optical band. This 17th magnitude knot ranks this as the second brightest extragalactic optical jet component, only slightly fainter than knot HST-1 of M87 despite its much greater distance. The optically-dominated SED of the bright knot (Fig. 5) is difficult to interpret; it may be best explained by IC from a decelerating relativistic jet aligned close to our line of sight and boosting downstream photons (Georganopoulos & Kazanas, 2003). Another possibility that cannot yet be ruled out is that this “knot” is actually an unrelated source. However, the SED and optical colors combined with a featureless (albeit low S/N) optical spectrum observed in

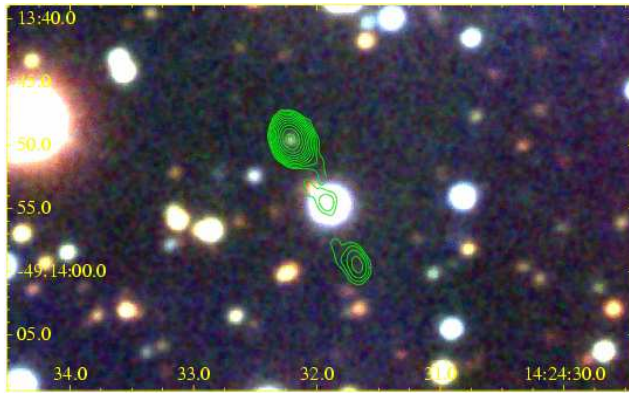


Figure 4: *Magellan* $g'-r'-i'$ true-color image of the PKS B1421–490 field, with 8.6 GHz radio contours.

April 2004 eliminates most contaminants except for an exotic, optically-dominated BL Lac object (Gelbord et al., 2005).

4 On the horizon...

This survey is very much a work in progress. A detailed report on the first 20 *Chandra* targets is coming out in January (Marshall et al., 2005). Of the remaining 36 sources in our sample, half have now been observed by us or by other investigators. Only by conducting large surveys will we discover unusual systems such as PKS 1421–490. We now have approved programs for follow-up *Chandra* and *HST* observations of selected sources. These data, together with new higher frequency radio observations, will provide the necessary data to examine the evolution of properties along the lengths of the jets through more detailed spatially-resolved SEDs. Our ground-based optical program is also continuing, with both imaging of systems not scheduled with *HST* and follow-up spectroscopy for 1421–490 and other sources with ambiguous identifications or unknown redshifts; the first collection of our *Magellan* results is due out next year (Gelbord & Marshall, 2005).

Acknowledgments

This work has been supported in part under SAO contracts GO4-5124X and SV1-61010. The Very Large Array is a facility of the National Radio Astronomy Observatory, operated by Associated Universities, Inc., under cooperative agreement with the National Science Foundation. The Australia Telescope Compact Array is part of the Australia Telescope which is funded by

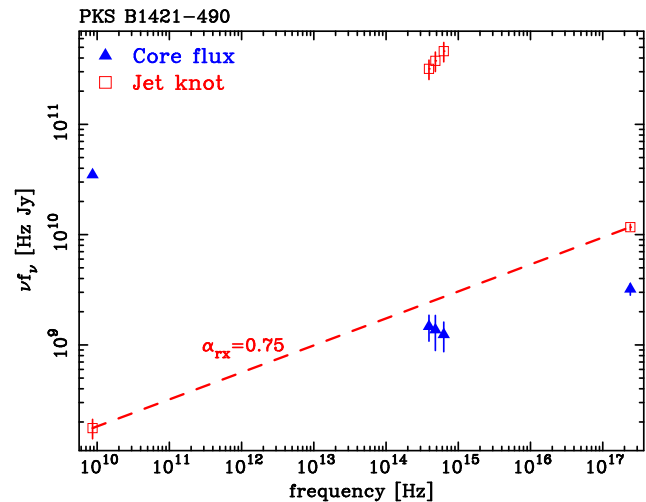


Figure 5: Radio–optical–X-ray SED of the core and knot of 1421–490.

the Commonwealth of Australia for operation as a National Facility managed by CSIRO.

References

- Celotti, A., Ghisellini, G., Chiaberge, M. 2001, MNRAS, 321, L1
- Dermer, C. D., Atayan, A. M. 2002, ApJ, 568, L81
- Gelbord, J. M., Marshall, H. L. 2005, in prep.
- Gelbord, J. M., et al. 2005, submitted to ApJL. Available online from <http://space.mit.edu/home/~jonathan/jets/>
- Georganopoulos, M., Kazanas, D. 2003, ApJ, 589, L5
- Harris, D. E., Krawczynski, H. 2002, ApJ, 565, 244
- Marshall, H. L., et al. 2001, ApJ, 549, L167
- Marshall, H. L., et al. 2005, ApJS, 156, 13
- Schreier, E. J., et al. 1979, ApJ, 234, L39
- Schwartz, D. A., et al. 2000, ApJ, 540, L69
- Schwartz, D. A., et al. 2003, New Ast. Rev., 47, 461
- Tavecchio, F., Maraschi, L., Sambruna, R. M., Urry, C. M. 2000, ApJ, 544, L23